quantum beam science

MDPI

Technical Note

Prototype Setup Hardware Choice for the DUCK System

Dmitriy Beznosko [1,*], Valeriy Aseykin [2], Alexander Dyshkant [3], Alexander Iakovlev [4], Oleg Krivosheev [5], Tatiana Krivosheev [1], Vladimir Shiltsev [3] and Valeriy Zhukov [2]

1 College of STEM, School of Sciences, Clayton State University, Morrow, GA 30260, USA; tatianakrivosheev@clayton.edu
2 P. N. Lebedev Physical Institute of the Russian Academy of Sciences, Moscow 119991, Russia
3 Department of Physics, Northern Illinois University, DeKalb, IL 60115, USA; dyshkant@nicadd.niu.edu (A.D.)
4 Upper School Science Department, Woodward Academy, College Park, GA 30337, USA; alex.iakovlev@woodward.edu
5 Xcision Medical Systems, Columbia, MD 21045, USA
* Correspondence: dmitriybeznosko@clayton.edu

Abstract: This article covers the overall design hardware choices for the prototyping activities for the DUCK (Detector system of Unusual Cosmic ray casKades). The primary goal of the DUCK system is to verify the existence of the unusual cosmic events reported by other collaborations and to look at the possibilities of adding innovations to the EAS (Extensive Atmospheric Shower) analysis methods of the EAS disk measurements at the observation level. Additionally, design and construction of the system provide educational experience to the students involved in the project and are developing the research capabilities of the university campus. The prototyping process has helped to choose between various design solutions in the process of optimizing of the individual detector components.

Keywords: cosmic rays; scintillator detectors; data acquisition systems

Citation: Beznosko, D.; Aseykin, V.; Dyshkant, A.; Iakovlev, A.; Krivosheev, O.; Krivosheev, T.; Shiltsev, V.; Zhukov, V. Prototype Setup Hardware Choice for the DUCK System. *Quantum Beam Sci.* **2024**, *8*, 17. https://doi.org/10.3390/qubs8030017

Received: 25 May 2024
Revised: 15 June 2024
Accepted: 27 June 2024
Published: 10 July 2024

1. Introduction

Cosmic Rays (CR) of ultra-high energy are currently of high interest, as CR studies are useful to understand the origin, propagations, and interaction of charged particles in our galaxy, as well as their interactions with the atmosphere and the formation of the EAS (Extensive Atmospheric Shower). CRs constitute a separate 'window' into space besides light and gravity. The DUCK (Detector system of Unusual Cosmic ray casKades) [1] system aims to contribute to the methodology of EAS event analysis and serve as an independent confirmation for detecting "unusual" CR events.

A typical EAS that is produced by the single ultra-high energy parent CR particle, from the point of view of the observer on the Earth surface, presents itself as a disk of various particle species that has variable thickness and particle density. As this disk passes through a particle detector, typically it will be recorded as a simple pulse with the duration corresponding to the disk thickness (and time it takes for it to pass the detector) and the area that is proportional to the particle density in that part of the disk.

However, starting around the 1950s, some EAS detection systems recorded events that had more than one pulse in a single detector. Originally, the name for such EAS detections was 'events with the delayed particles' as the hypothesis that tried to explain multiple pulses suggested that if a heavy particle is produced during EAS development, it will have a lower speed and thus will lag behind the disk. As it decays, it will produce its own disk, so the detector will report this as two subsequent pulses (or more). The first detailed description of this work was published by J. Jelley and W. Whitehouse in 1953 [2]. Various research groups and collaborations, mostly from the US and UK, in the 1960s–1980s have focused on such delayed particle events [3–5]. Since the 1970s, Japan has also joined this search [6,7]. Detectors were built, and work was carried out at Moscow State University (MSU) [8,9] and at LPI (TSHASS) [10,11] around the 1980s and after that as well.

As technology developed, it became clear that these 'delayed particle' events come with several maxima, not just two. Such events have been recorded since the 1990s at the facility in Yakutsk [12] and in the 2000s at the "Tunka" system (MSU) [13]. The results from all these works are not clearly conclusive and do not match. This suggests that further studies of such events are needed.

Numerous events with multiple maxima have been recorded by the Horizon-T [14] detector system, where they are called the 'unusual' CR events. This pursuit of the DUCK system to study check events further represents a vital step towards unraveling the mysteries of CR and their profound impact on our understanding of the universe. Additionally, as the detector system is being designed and built at Clayton State University, which is designated as a MSI (minority serving institution), this work helps to promote the research to multiple minority groups that are underrepresented in the STEM field.

The current design of the DUCK builds on the original proposal [15] and considers both the need for high-speed digitization of the signals as well as the nanosecond-level time resolution that is needed to study the applicability of the EAS disk width to the data analysis and the simulation checking for this parameter as well.

2. Prototype Design

Each module of the detector system should be able to detect individual cosmic muons for detector response calibration purposes and have a large dynamic range at the same time as the particle density in the EAS disk varies significantly. The response of the detector to a single particle is a pulse of a finite width, so the resolution of the detector is dependent on the width of this pulse. In order to resolve a group of particles that come in rapid succession as individual signals, this width should be as short as possible.

The design of the prototype module is a truncated pyramid (the shape is adopted from [16] following the Horizon-T choice) with the Hamamatsu [17] H11284-30 (former R7723) PMT at the top and the plastic scintillator ($0.5 \times 0.5 \times 0.024$ m^3) at the bottom. A completed module is shown in Figure 1a. The PMT photocathode is looking directly at the scintillator, and it is about 55 cm above the scintillator for the prototype and will be about 1 m above for the final design, all enclosed in the light-tight case. This ensures increased uniformity of the PMT response to the particles passing through different parts of the scintillator, as shown in [16]. Figure 1b shows the schematic with the PMT and the secondary Hamamatsu 1.3 mm^2 Multi-Pixel Photon Counter (MPPC) photosensor placement positions. The MPPC sensor will have a wavelength-shifting (WLS) optical fiber with peak emission in green (475 nm, Y11 fiber) attached to it to facilitate light collection. The fiber will be placed directly under the scintillator. The interior and exterior are lined with foil; on the inside, the bottom part, and the walls are initially covered by Tyvek [18]. The entire system output is recorded by the CAEN [19] DT5730 Flash Analog-to-Digital Converter (FADC).

This ADC has a 14-bit resolution and a 500 MHz digitization rate and is thus suited for particle detection at ns-scale time resolution. Additionally, this ADC can record events from about 10 µs to around 10 ms long with an acquisition memory of 5.12 MS/ch. When a lower event duration is chosen, this memory acts as the data buffer. Note that since the PMT has an intrinsic spread of the pulse of about 1.8 ns, a higher ADC digitization frequency will not add benefits to the detected signal and will raise the overall cost. Also, DT5730 can be connected via USB2 port and is a stand-alone model that does not require any crate or external power, etc. Several modules can be synchronized using the external clock generator if needed.

The MPPC and LED are the elements of the module calibration system that still need to be tested with the fully completed module. The LED is connected to Rigol [20] DG2102 Waveform Generator. These elements have not yet been fully implemented at the time of this article and are under final construction and testing.

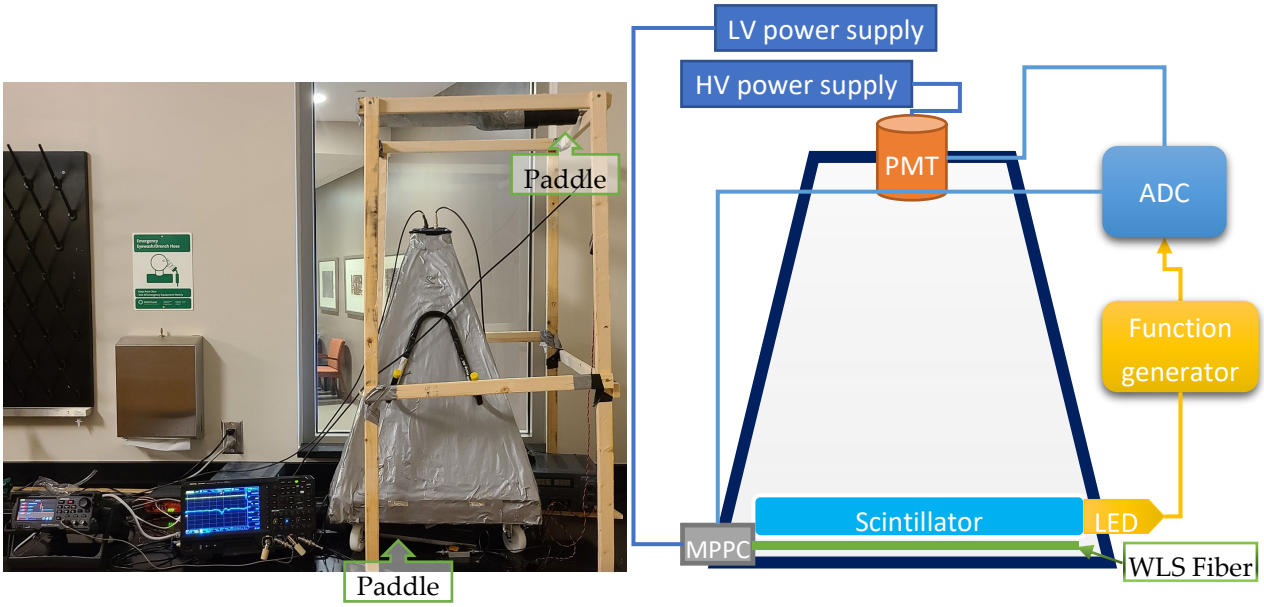

(**a**) (**b**)

Figure 1. (**a**) Completed prototype module under testing with paddle detectors; (**b**) Updated design schematic of the DUCK detector module prototype.

Paddles Design and Construction

To make sure that the particle passes through the detector, a double-coincidence scheme is used. For that, two simple detectors are needed that are placed above and under the module under testing. The most common simple detectors are called paddles, which are just a flat piece of the scintillator coupled with the PMT. These scintillator paddles form the hodoscope for the cosmic muon coincidence scheme for the prototype calibration. Each paddle is manufactured from a 2.4 cm-thick scintillator, with the square part of the paddle being about 25 cm $\times$ 35 cm. The PMT holder that attaches to the case is 3D-printed. The scintillator on the bottom side has a layer of Tyvek for higher light yield. Additionally, aluminum foil, insulation tape, and duct tape were added for both light insulation and structural support. Figure 2a shows the completed paddle, and Figure 2b shows all the layers exposed before completion. The same model PMTs are used for the detector modules. These two paddles were constructed for use in a double coincidence scheme to be used for the detector system's individual module calibration. The paddles will be placed above and under each module for this process, as shown in Figure 1a. The paddles are smaller than the module size, this way, different parts of the module can be calibrated as the detector response uniformity can be estimated.

(**a**) (**b**)

Figure 2. (**a**) Completed paddle detector; (**b**) Construction stages, showing the PMT holder, Tyvek, aluminum foil and insulating tape layers.

The polystyrene-based scintillator EJ-200 from Eljen [21] will be used for the final modules. As for the prototype, before EJ-200 was placed in it, it was initially tested with existing lab pieces of the generic scintillator with the PPO (2,5-Diphenyloxazole) fluor and POPOP (1,4-bis(5-phenyloxazol-2-yl) benzene) shifter with the characteristics shown in [22]. The PMT is optimized for blue light detection, but the scintillator material produces UV light. Fluor and shifter convert this UV light into blue (with a wavelength of around 410 nm or so; see [22] for details).

With the paddles connected to the oscilloscope, the 'Setup and Hold' trigger option can be used to set up the two-level coincidence between the paddles for reliable cosmic muon detection. For the ADC, other options are available, as described later in this paper.

3. Detector and Paddles Initial Calibration

3.1. PMT Calibration

The first test that was conducted on the newly constructed detectors was to determine the optimal bias voltage for the PMT as well as to set the initial threshold at that bias voltage. PMT, just like any photon detector, has intrinsic noise that can affect the detection. Also, each PMT is different and thus requires a separate biasing voltage to be set individually. There is an interplay between the noise and detection efficiency, as the detection efficiency and noise increase with the bias voltage. Thus, the optimal values of both need to be determined.

For this test, the detector in question is connected to the signal counter (or scaler) via the discriminator. We have used the Rigol MS5A231000594 oscilloscope as it has a counter with the variable threshold already built in. The count values are recorded at different bias voltages and threshold values and then plotted. Figure 3 is a sample plot of the log of the average number of counts per second (i.e., average frequency) vs. the threshold value for different biases for the detector prototype module shown as an example. As the threshold is increased for the same bias voltage, first the noise is reduced, then the actual CR signal counts start to be cut by further threshold increases. The region where the fast-decreasing noise counts transition into the CR counts can appear as either a short horizontal line or form a rather large plateau. The threshold is typically chosen at the beginning of the plateau (i.e., the right side of it) for a given bias so as to keep the CR signal as some noise can be tolerated as described next.

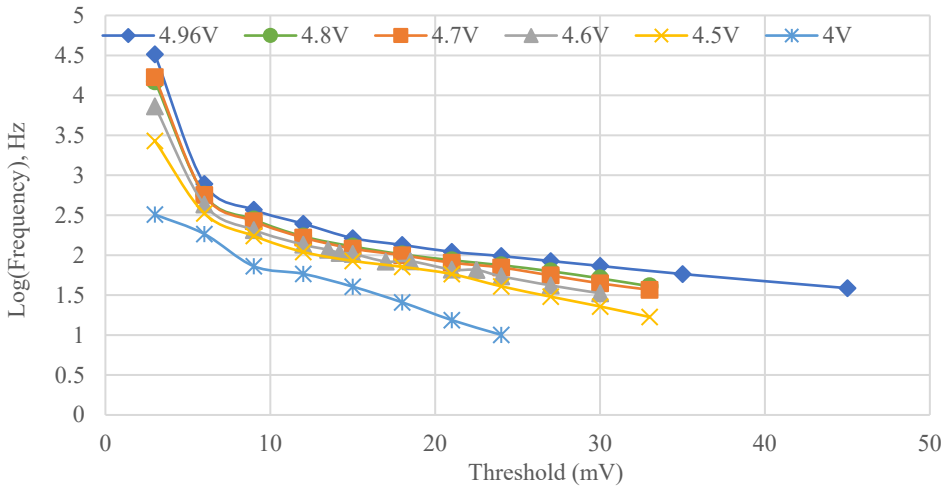

Figure 3. Count frequency at different threshold values and bias voltages.

Figure 3 lists the voltage as it is read by the power supply monitor. The cable connecting both is around 30 cm, so the loss is insignificant. Normally, the PMT draws the current below the power supply rating, and the value at the PMT is effectively the same as at the monitoring. When very high signals are detected by the PMT, the voltage can drop,

and this will limit the overall PMT linearity, as has been shown in in the detailed studies described in [16]. The current test is not affected by this effect.

The frequency of the noise is important for the double coincidence triggering scheme, as within the coincidence window, two noise signals can randomly appear, creating a false detection of the cosmic event. For this case, the frequency of these false triggers can be estimated using Equation (1):

$$f_{False} = f_{noise_1} \times f_{noise_2} \times 2w_{coin} \quad (1)$$

Here, f_{noise} is the average noise of each paddle (in Hz) for the threshold and bias values chosen, and w_{coin} is the width of the coincidence window in seconds. With the typical noise around 300 Hz and the coincidence window of about 50 ns (adjustable), the rate of these false coincidences will be around 1 event in 500 s. As the measured rate of the CR muons with the paddle detectors is on the order of a few events per second, this rate of false coincidences is acceptable.

3.2. Initial Calibration with Cosmic Rays

A very important detector calibration and performance assessment test is conducted using the Minimally Ionizing Particles (MIP), which are typically cosmic ray muons. To conduct this test, two paddle detectors are placed above and below the detector being tested, and the FADC is set to detect the double coincidence events as defined by these paddles. Then, data are analyzed to determine various properties of the detector response to the MIP signal, such as a sample amplitude as shown in Figure 4. The resulting histogram is fitted with a Landau curve to determine the MPV (Most Probable Value) for the distribution. The calibration process is ongoing, and the detailed parameters of each detector module will be published at a later time. As FADC has a range of 2 V and a resolution of 14 bits, the value in ADC bins should be divided by 2^{13} to get the amplitudes in volts.

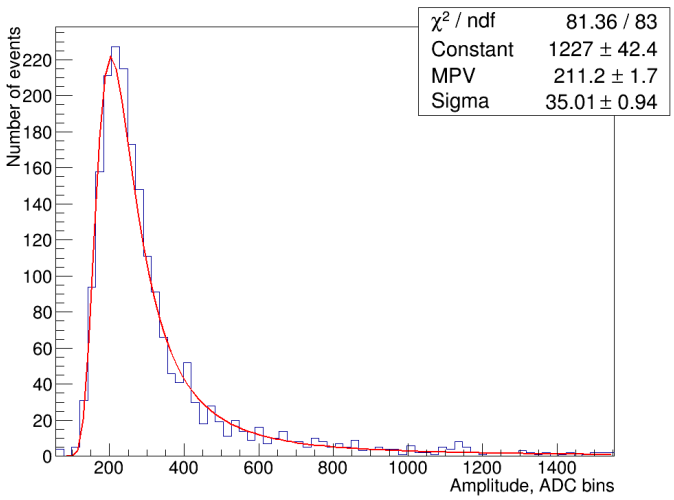

Figure 4. The amplitude of the detector response to MIP. Red line is a fit using Landau curve.

4. Operating ADC–DAQ Software

Special software has been designed to control the DT5730 ADC. The considerations that went into the software architecture were to provide a high-speed readout and the ability to control all ADC functions, as well as provide a real-time even display that can show the data being recorded while giving priority to data retrieval and saving over the display.

The software utilizes the TBB (tread building blocks) library to create the asynchronous queue of data. A single thread is tasked with checking the ADC to see if new data are available and retrieving this data. The queue served as an additional buffer in case there was a burst of events from the detector.

Another thread takes events at an adjustable time interval from the queue, makes a copy, and draws it (Figure 5). This way, only a sampling of data is displayed, so the software can be run on older computers with lower CPU and graphics capabilities without losing its main functionality

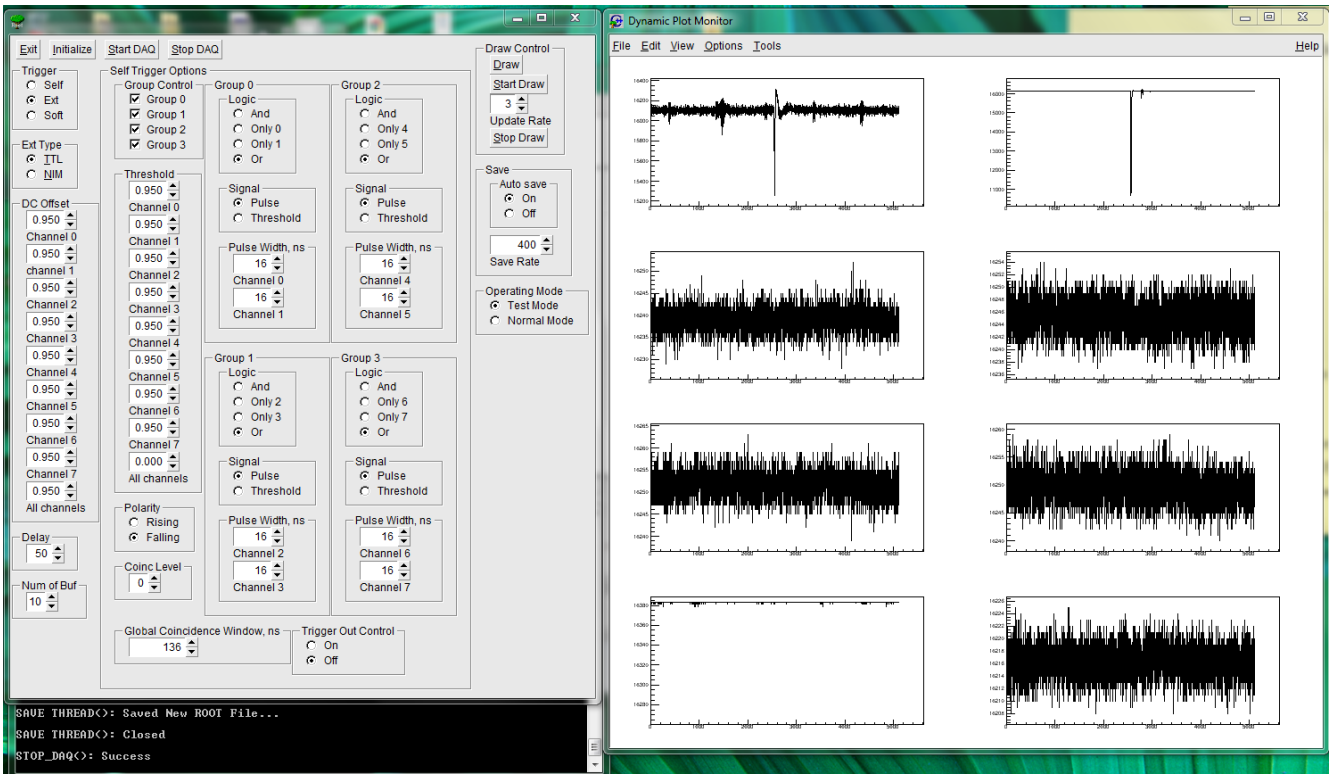

Figure 5. The DAQ software control panel interface and the data display showing live data from FADC channels 0 to 7.

Another feature is the ability to save events in a file by groups—from 1 per file to hundreds of thousands, limited to 2 Gb per file. The limitation comes from the library used in ROOT version 5.34/38 [23], which saves the data as a tree structure that allows for quick access to any event, even in a large file—no need to read the whole file sequentially. Data are also zipped on-the-fly to reduce the size of the file. The same control allows you to stop saving data for testing purposes.

The control panel interface shown in Figure 5 allows to set the trigger type—Soft means random trigger by software, Ext means accepting the externally generated trigger in either NIM or TTL format, Self—the ADC will generate the trigger itself.

The rest of the interface deals with setting the parameters for the self-triggering option. One can set the threshold for each channel and set the triggering of the channel group (channels 0–1, 2–3, 4–5 and 6–7 are in four groups). Pulse width sets the coincidence window in Equation (1)—how many ns will the ADC wait after the threshold is reached for the second pulse before giving up. The number of buffers controls the number of points in each event—from 5111 to the higher number of buffers (the actual number is 2 to the power of 10), and the number of points in each event doubles with the reduction in the number of buffers—i.e., 10222 for 2^9, etc. The coincidence level sets the global coincidence between channel groups—how many groups must report a signal before the global trigger is issued.

The data displayed shows the window for each FADC channel, with the data shown as amplitude in ADC bins vs. time in ns. Effectively, this operates like an oscilloscope screen and allows for real-time monitoring of the data during the run.

5. Conclusions

In conclusion, the design and prototyping of the DUCK system have demonstrated the operations that meet the expected characteristics. The prototyping process is providing valuable insights for the final design, such as the scintillator choice and thickness and calibration processes. Additionally, the procedure for PMT calibration has been set and will be used to determine the most optimal thresholds and voltages for our data collection in the final design as well. In order to develop and test the DAQ software, as well as to support students educational experience and demonstrate the use of particle physics methods in other areas, the DUCK prototype hardware was also used to execute the project on random numbers with the details described in [24].

Author Contributions: Conceptualization, D.B., V.A., V.S. and V.Z.; methodology, A.D. and V.A.; software, O.K.; validation, A.D., T.K. and A.I.; formal analysis, D.B.; investigation, D.B.; resources, D.B. and A.I.; data curation, T.K.; writing—original draft preparation, D.B.; writing—review and editing, A.D., T.K. and A.I.; visualization, D.B.; supervision, D.B.; project administration, D.B.; funding acquisition, D.B. All authors have read and agreed to the published version of the manuscript.

Funding: This work is supported by the NSF LEAPS-MPS Award 2316097.

Conflicts of Interest: Author Oleg Krivosheev was employed by the company Xcision Medical Systems. The remaining authors declare that the research was conducted in the absence of any commercial or financial relationships that could be construed as a potential conflict of interest. Xcision Medical Systems had no role in the design of the study; in the collection, analyses or interpretation of data; in the writing of the manuscript; or in the decision to publish the results.

References

1. Beznosko, D.; Aseykin, V.; Dyshkant, A.; Iakovlev, A.; Krivosheev, O.; Krivosheev, T.; Zhukov, V.V. DUCK Detector System Design. In Proceedings of the 38th International Cosmic Ray Conference (ICRC2023), Nagoya, Japan, 26 July–3 August 2023. PoS(ICRC2023)187. [CrossRef]
2. Linsley, J.; Scarsi, L. Arrival times of air shower particles at large distances from the axis. *Phys. Rev.* **1962**, *128*, 2384. [CrossRef]
3. Baxter, A.J.; Watson, A.A.; Wilson, J.G. Shower front structure and the properties of extensive air showers. In Proceedings of the 9th ICRC, London, UK, September 1965; Volume 1, pp. 724–726.
4. Mincer, A.I.; Freudenreich, H.T.; Goodman, J.A.; Tonwar, S.C.; Yodh, G.B.; Ellsworth, R.W.; Berley, D. A study of arrival time structure of low energy hadrons near air shower cores at sea level. In Proceedings of the 18th ICRC, Bangalore, India, 22 August–3 September 1983; Volume 11, pp. 264–267.
5. Hara, T.; Hatano, Y.; Hayashida, N.; Ishikawa, F.; Jogo, N.; Kamata, K.; Kifune, T.; Nagano, M.; Ohno, Y.; Ohoka, H.; et al. The Akeno air shower project. In Proceedings of the 16th ICRC, Kyoto, Japan, 6–18 August 1979; Volume 8, pp. 135–140.
6. Inoue, N.; Kawamoto, M.; Misaki, Y.; Maeda, T.; Takeuchi, T.; Toyoda, Y. Structure of air shower disk near the core. In Proceedings of the 19th ICRC, La Jolla, HE, USA, 11–12 August 1985; Volume 7, pp. 316–319.
7. Atrashkevich, V.B.; Vedeneev, O.V.; Garipov, G.K.; Kalmikaov, N.P.; Kulikov, G.V.; Silayev, A.V.; Solov'eva, V.V.; Sulakov, V.P.; Fomin, Y.V.; Khrenov, B.A.; et al. Delayed pulses in EAS at sea-level. *Bull. Russ. Acad. Sci. Phys.* **1994**, *58*, 98–102.
8. Kulikov, G.V.; Fomin, Y.A.; Garipov, G.K.; Kalmykov, N.N.; Khrenov, B.A.; Kulikov, G.V.; Kuzmuchev, L.A.; Lidvansky, A.S.; Nazarov, V.I.; Panasyuk, M.I.; et al. Complex EAS array for super-hight energy cosmic ray research. In Proceedings of the 28th ICRC, Tsukuba, Japan, 31 July–7 August 2003; Volume 1, pp. 973–976.
9. Beisembaev, R.U.; Vavilov, Y.N.; Dedenko, L.G.; Kruglov, A.V.; Stepanov, A.V.; Takibaev, Z.S. Investigation of the arrival time distribution of muons with energy $\geq$5 GeV in EAS at mountain level (690 g/cm^2). In Proceedings of the 24th ICRC, Rome, Italy, 28 August–8 September 1995; Volume 1, pp. 454–457.
10. Beisembaev, R.U.; Vavilov, Y.N.; Vildanov, N.G.; Kruglov, A.V.; Stepanov, A.V.; Takibaev, J.S. Delayed Muons in extensive air showers and double-front showers. *Phys. At. Nucl.* **2009**, *72*, 1852–1859. [CrossRef]
11. Glushkov, A.V.; Kosarev, V.B.; Makarov, I.T.; Sleptsov, I.E.; Filippov, S.A. Temporal structure of the muon disk at large distances from the axis of extensive air showers with E 0$\geq$6 $\times$1016 ev. *JETP Lett.* **1998**, *67*, 383–388. [CrossRef]
12. Budnev, N.M.; Wishnevski, R.; Gress, O.A.; Zabolotsky, A.V.; Zagorodnikov, A.V.; Kalmykov, N.N.; Kozhin, V.A.; Korosteleva, E.E.; Kuzmichev, L.A.; Lubsandorzhiev, B.K.; et al. Tunka-133: Status 2008 and development of methods for data analysis. *Bull. Russ. Acad. Sci. Phys.* **2008**, *73*, 588–592. [CrossRef]
13. Budnev, N.M.; Chiavassa, A.; Gress, O.A.; Gress, T.I.; Dyachok, A.N.; Karpov, N.I.; Kalmykov, N.N.; Korosteleva, E.E.; Kozhin, V.A.; Kuzmichev, L.A.; et al. The primary cosmic-ray energy spectrum measured with the Tunka-133 array. *arXiv* **2021**, arXiv:2104.03599v1. [CrossRef]

14. Beisembaev, R.U.; Baigarin, K.A.; Beznosko, D.; Beisembaeva, E.A.; Vildanova, M.I.; Zhukov, V.V.; Petlenko, M.S.; Ryabov, V.A.; Sadykov, T.K.; Shaulov, S.B. The Horizon-T cosmic ray experiment. *Nucl. Instrum. Methods Phys. Res. Sect. A Accel. Spectrometers Detect. Assoc. Equip.* **2022**, *1037*, 166901. [CrossRef]
15. Beznosko, D.; Aseykin, V.; Dyshkant, A.; Iakovlev, A.; Krivosheev, O.; Krivosheev, T.; Zhukov, V.V. Design Considerations of the DUCK Detector System. *Quantum Beam Sci.* **2023**, *7*, 6. [CrossRef]
16. Beznosko, D.; Beisembaev, R.U.; Beisembaeva, E.A.; Duspayev, A.; Iakovlev, A.; Sadykov, T.X.; Uakhitov, T.; Vildanova, M.I.; Yessenov, M.; Zhukov, V.V. Fast and simple glass-based charged particles detector with large linear detection range. *J. Instrum.* **2017**, *12*, T07008. [CrossRef]
17. Hamamatsu Photonics, K.K. Electron Tube Division. Available online: http://www.hamamatsu.com (accessed on 26 June 2024).
18. Uline. Available online: https://www.uline.com/BL_1969/Tyvek-Rolls (accessed on 26 June 2024).
19. CAEN, S.p.A. Via della Vetraia, 11, 55049 Viareggio Lucca, Italy. Available online: https://www.caen.it/ (accessed on 26 June 2024).
20. Rigol Technologies, 10220 SW Nimbus Ave. Suite K-7 Portland, OR 97223. Available online: https://www.rigolna.com/ (accessed on 26 June 2024).
21. Eljen Technology, 1300 W. Broadway Sweetwater, Texas 79556, United States. Available online: https://eljentechnology.com/ (accessed on 26 June 2024).
22. Beznosko, D.; Holloway, E.; Iakovlev, A. Optimization of the Composition of Toluene-Based Liquid Scintillator. *Instruments* **2022**, *6*, 56. [CrossRef]
23. Brun, R.; Rademakers, F. ROOT—An object oriented data analysis framework. *Nucl. Instrum. Methods Phys. Res. Sect. A Accel. Spectrometers Detect. Assoc. Equip.* **1997**, *389*, 81–86. [CrossRef]
24. Beznosko, D.; Driscoll, K.; Guadarrama, F.; Mai, S.; Thornton, N. Data Analysis Methods Preliminaries for a Photon-based Hardware Random Number Generator. *arXiv* **2024**, arXiv:2404.09395.